Physical Science International Journal
11(3): 1-15, 2016, Article no.PSIJ.27900
ISSN: 2348-0130

SCIENCEDOMAIN *international*
www.sciencedomain.org

Energy Generation Using Thermoelectric Power Generator (TEPG) from the Living Body

A. R. M. Siddique[1*] and S. H. Majid[2]

[1]School of Engineering, University of Guelph, Guelph, Ontario N1G 2W1, Canada.
[2]Department of Electrical Engineering, University of Tabuk, Saudi Arabia.

Authors' contributions

This work was carried out in collaboration between the two authors. Author ARMS designed, analyzed and experimentally tested this research work under the supervision of author SHM. The first draft of the manuscript was written by author ARMS and then it was reviewed and edited by author SHM. The two authors read and approved the final manuscript.

Article Information

DOI: 10.9734/PSIJ/2016/27900
Editor(s):
(1) Junjie Chen, Department of Electrical Engineering, University of Texas at Arlington, USA.
(2) Stefano Moretti, School of Physics and Astronomy, University of Southampton, UK.
Reviewers:
(1) Giovanna Scarel, James Madison University, Harrisonburg, USA.
(2) Anonymous, Chungbuk National University, Korea.
(3) Wen-Yeau Chang, St. John's University, Taiwan.
Complete Peer review History: http://www.sciencedomain.org/review-history/15739

Original Research Article

Received 24th June 2016
Accepted 1st August 2016
Published 10th August 2016

ABSTRACT

In this paper, a general idea about wearable thermoelectric generator from the body heat has been discussed. First, a thermoelectric generator, which is usually used for industrial purposes (Tellurex-G2-40-0329 series), was used for lab experiment to observe the output results at the low-temperature difference (i.e., ΔT=6-18 K). At this temperature range, the power output was approximately 0.0192-0.35 µW which was very low for practical use. Different configurations of TEG (single, double, single TEG with fin, etc.) were used to find out the best one, which could generate maximum power. It is found that a single thermoelectric generator with a fin can harvest a maximum power output of around 2.5 µW. A list of low temperature-based, thermoelectric n-type and p-type materials was presented. *n*-type 75% Bi_2Te_3, 25% Bi_2Se_3 and *p*-type 25% Bi_2Te_3 0.75% Sb_2Te_3 (1.75%Se) were used for numerical and finite element analysis for wearable thermoelectric generator. A maximum of 6.5 µW power can be harvested from body heat when body temperature is 37℃ and the ambient temperature is considered as 25℃ (ΔT =12 K) for this thermoelectric element. Maple, FlexPDE, and SolidWorks were used for numerical analysis and finite element analysis (FEA).

**Corresponding author: E-mail: asiddi04@uoguelph.ca;*

Keywords: Thermoelectric generator; wearable TEG; seebeck effect; figure of merit; thermal resistance.

1. INTRODUCTION

Over the last two decades, advancements in microelectromechanical system (MEMS) and miniaturization of electronic devices have lowered the consumption of electrical energy in the range between miliwatts (mW) to microwatts (μW). Devices which fall in to this level of energy consumption are becoming more suitable to be used in wireless sensor networks (WSN) [1]. The chemical batteries which have a finite lifetime and have biohazard impact on the environment. On the other hand these batteries require extra labor for replacement [2]. Therefore, researchers are trying to overcome this energy management with alternative energy sources (i.e., renewable energy sources). However, traditional renewable energy sources are much larger in size, require costly initial set-up, and are not suitable for microelectronic devices [3]. Therefore, the thermoelectric power generator (TEG) is one of the most attractive solutions for fulfilling the power demand of mobile electron devices.

From 2000 till to-date, a large number of researches have been conducted and are still being developed. The idea of this research is to develop the energy harvesting technology through TEG. The first practical thermoelectric module was introduced in 1960s. Since then it has been used for harvesting power, cooling, pumping and heating applications [4]. The first TEG that used body heat was fabricated and used in a shirt in 2009 [5]. Over the last decade, starting from 2005, many researchers from all over the world have done many theoretical, simulation-based and practical experiments on TEGs to harvest energy from the human body.

Leonov et al. [6] discussed the power generation capability of the human body and found out that the forehead is the most suitable location to harvest energy using TEG. The outputs of their developed devices were 30-70 μW from the body heat. Mitcheson [7] compared the kinetic power generator and TEG and reported that the generation efficiency is better for the kinetic energy harvester even though the thermoelectric generator is suitable for wireless sensors, powered by the body heat. The power density was 20 μW/cm^2 during running, whereas it was 10 μW/cm^2 during walking. In 2010, Lossec et al. [8] proposed to improve the power generation by introducing a new factor, $Z_{E,}$ and using DC-DC converter for TEG. TEG module TM-450.0.8.3.0 was used for their experiments and showed that it can generate 7 μW/cm^2, with a heat sink while normal walking and 30 μW/cm^2 while running. Leonov presented that human body has a high thermal resistance, which has an effect on the design of TEG [9]. After the close observations through the experiments, it was mentioned that thermal resistance of the TEG should be hundreds of cm^{2}kW^{-1}.

Jo et al. [10] proposed dispenser-printing technology for TEG developed by a polydimethylsiloxane (PDMS) substrate, which made it flexible and had a low thermal conductivity. The power output of TEG was 2.1 μW at 19 k. Suemori et al. [11] used very light weight composite materials i.e., polystyrene and carbon nanotubes as a thermoelectric (TE) materials for their proposed TEG. It was developed on polyethylene naphthalate film using printing technology. The prototype can generate 55 mW/m^2 at 70 K temperature difference. Kim et al. [12] designed a wearable TEG, which consisted of 12 couple of $Bi_{0.5}Sb_{1.5}Te_3$ and $Bi_2Se_{0.3}Te_{2.7}$ materials those were fabricated on polymer based fabric. The power and voltage outputs were 224 nW and 14.2 mV at 15 K temperature difference. Kim et al. [13] designed a glass-fabric based flexible-TEG using printing process with *n*-type Bi_2Te_3 and *p*-type Sb_2Te_3 TE materials. The power density of the prototype is 3.8 mW/cm^2 at 50 K.

Typical TEGs are used for industrial purpose where there is a huge temperature difference between two surfaces of the TEG. Therefore, the wearable thermoelectric power generator (WTEPG) is becoming a new platform for wireless sensor networks to provide the green, less costly, and energy efficient power. WTEGs are attached to the human body to harvest the thermal energy and convert it into electrical energy. Normally the human body temperature is around 37℃ [9] whereas the ambient temperature is not fixed. It varies randomly around the world and hourly basis as well. For this research, the range of ambient temperatures is considered from 19℃ to 31℃. However, most of the TEGs available in the market are designed for high temperature (typically $\Delta T > 50$℃), which is not suitable for harvesting energy from body heat. Therefore, one of the objectives of this research work is to determine if the commercial

TEGs are used for harvesting energy from the human body what will be the power output. Moreover, another objective is to investigate the properties of thermoelectric materials, which are suitable at low temperature (ΔT= 6-18℃) and analyze their behavior.

2. THERMOELECTRIC GENERATOR

TEG is a solid-state static device. TEG generates electrical energy from thermal energy due to the temperature difference across its two surfaces. Thomas Johann Seebeck first discovered this technology in 1821 [14]. This energy harvesting technology is environmentally friendly. The size of the TEG varies from mili (m) to micro (μ) range, no maintenance cost is required, and has 20-30 years of an operational lifetime which has made this technology very popular nowadays. Recently, TEGs are used in many applications including micro self-powered wireless platforms, industrials areas, hot pipelines, aircrafts, biosensors, automobiles, the human body, telemetry systems, in the internal combustion engine as a heat recovery device, and in small electronic devices for various applications. Especially, in coming decades, tracking, monitoring sensors and surveillance system of health are going to be expanded very quickly, which is one of the big largest platforms of mobile sensor networks.

2.1 Wearable TEG

WTEPG is nothing but a specially designed TEG, which uses the temperature difference of any living body and surrounding temperature to harvest energy. The human body is a great source of energies such as heat, motion, and vibration. These energies can be used to convert into electrical energy. Therefore, WTEG can be used to convert this heat energy into electrical energy.

2.2 Basic Principal

The fundamental principle of TEG is based on the Seebeck effect of TE materials. It can generate voltage if there is a temperature gradient between two sides of the element. According to the Seebeck effect, the generated voltage is directly proportional to the temperature difference.

$$V = \alpha \Delta T \tag{1}$$

where, α is the Seebeck coefficient of the materials. A typical value of Seebeck coefficient of commercially used n-type material Bismuth Telluride (Bi_2Te_3) is 287×10^{-6} V/K at 54℃ and for p-type material Antimony Telluride (Sb_2Te_3), it is $101\text{-}161\times10^{-6}$ V/K at room temperature [15,16].

A thermoelectric element consists of p-type and n-type semiconductors where p-type has excess holes and n-type have excess electrons to carry the energy. Typically, a large number of TE materials are connected electrically in series to increase the generation of voltage and thermally in parallel for increasing the thermal conductivity. The standard size of TEG modules is vary from 4 mm × 4 mm× 3 mm to around 50 mm × 50 mm × 50 mm [17]. Fig. 1 illustrates a typical single thermoelectric cell.

The thermal efficiency of thermoelectric materials depends on the figure of merit (Z). The typical value for ZT (dimensionless unit, T is the temperature in K) is around 1 [18] for most materials such as for Bi_2Te_3 is 0.8 at room temperature [19]. This figure of merit depends on:

$$Z = \frac{\alpha^2}{\rho k} \tag{2}$$

where, ρ is electrical resistivity and k is thermal conductivity. The Power generation from thermoelectric module not only depends on these parameters but also depends on area ($A_t = A_n + A_p$, here A_t is total area, A_n is cross-sectional area of n-type materials, A_p is cross-sectional area of p-type materials) of the one pair, length of the materials lag (l), hot surface and cold surface temperature of TEG module (T_{Hs} and T_{Cs}), internal electrical resistance of the materials (R_{in}) and number of couples (n) in one module as well.

2.3 Mathematical Modeling of TEG

The difference between the rate of heat energy entering the hot side Q_H and going out from the cold side of the module Q_C is the amount of generated power (P) by the module.

$$P = n(\dot{Q}_H - \dot{Q}_C) \tag{3}$$

where,

$$\dot{Q}_H = n[\alpha I T_{Hs} + K(T_{Hs} - T_{Cs}) - 0.5 I^2 R_{in}] \tag{4}$$

$$\dot{Q}_C = n[\alpha I T_{Cs} + K(T_{Hs} - T_{Cs}) + 0.5 I^2 R_{in}] \tag{5}$$

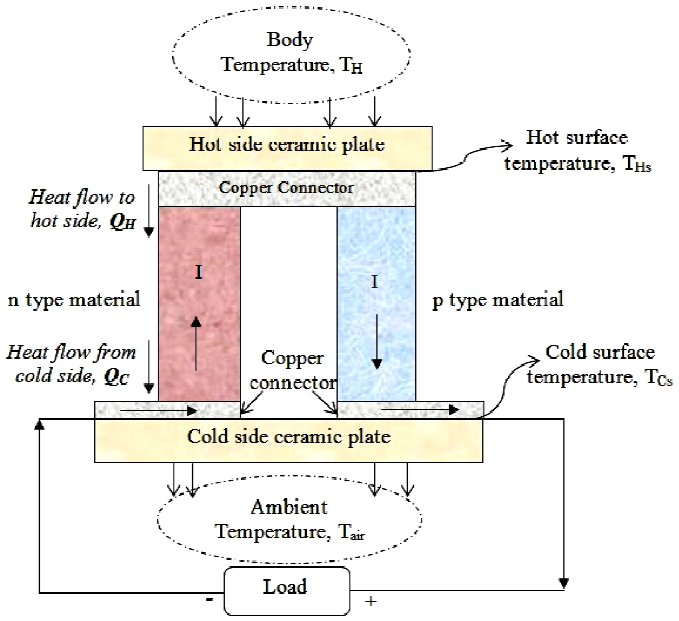

Fig. 1. Schematic diagram of a thermoelectric pair with *n*-type and *p*-type TE leg

In equation (4) and (5), $\alpha = (\alpha_n + \alpha_p)$, α_n and α_p are the Seebeck coefficients of *n*-type and *p*-type materials, respectively and the thermal conductance *K* is given by:

$$K = k_n\gamma_n + k_p\gamma_p \tag{6}$$

where,

$$k_n = \frac{\alpha_n^2}{\rho_n Z_n} \tag{7(a)}$$

$$k_p = \frac{\alpha_p^2}{\rho_p Z_p} \tag{7(b)}$$

$$\gamma = \frac{Area}{length} = \frac{A}{l} \tag{7(c)}$$

where, k_n and k_p are the thermal conductivities, γ_n and γ_p are the ratios of the area to the length, ρ_n and ρ_p are the electrical resistivities, Z_n and Z_p are the figures of merits of *n*-type and *p*-type materials, respectively. Internal resistance of the module is calculated by:

$$R_{in} = \frac{\rho_n}{\gamma_n} + \frac{\rho_p}{\gamma_p} \tag{8}$$

3. EXPERIMENTAL TESTS AND RESULTS

A commercial TEG module (Tellurex, G2-40-0329 series) was used for the experiment in the lab. Bi-Te based thermoelectric materials are used in this module which is designed for industrial purposes. It can generate maximum power when hot side temperature is 250℃ and cold side is 50°C. But for this lab experiment, low temperatures were used. The specification and testing parameters are given in Table 1 and Fig. 2 shows the experimental setup.

In this experiment, a thermo-regulator was used for circulating hot water through the heat exchanger plate, which can be considered as a human body. Different temperatures can be set in the thermo-regulator to change the plate temperature because the ambient temperature is fixed in the lab. The resistance of 3.3 Ω was used as a load in the external circuit to match with an internal resistance of the module. A Multimeter was used for measuring the generated voltage and current. A thermometer was used for measuring the plate and ambient temperatures. Three different cases were considered for experimental tests and for comparing the results to determine the optimum case for harvesting maximum power.

3.1 Single TEG Module

At first, only one TEG module was used for the experiment. Fig. 3 shows the single module of Tellurex G2-40-0329 series.

Table 1. Parameters used for the experimental test [20]

Specification	Value
Hot surface temperature, T_H	37℃
Ambient temperature, T_{air}	19-31℃
Module size	4 mm × 4 mm × 3.5 mm
Internal Resistance of TEG, R_{in}	3.1 Ω
Seebeck coefficient of n-type, α_n	225×10^{-6} V/K
Seebeck coefficient of p-type, α_p	230×10^{-6} V/K
Thermal resistivity of n-type, ρ_n	1.3×10^{-5} ohm-cm
Thermal resistivity of p-type, ρ_p	1.27×10^{-5} ohm-cm
Thermal conductivity of n-type, k_n	1.14 Watt/cm.K
Thermal conductivity of p-type, k_p	1.14 Watt/cm.K
Total area, A_t	1.96 mm^2
Length, l_n=l_p	1.4 mm
Thickness of the copper plate	0.3 mm
Gap between two lags	1.08 mm
Number of Couples, n	128
Load resistance, R_L	3.3 Ω

Fig. 4 represents the experimental results of open circuit voltage and short circuit current at different temperature gradients (6-18℃). The open circuit voltage and short circuit current increase with increasing temperature difference between hot surface and the ambient temperature. Therefore, the output power also increases.

Fig. 5 indicates the matched load voltage, load current and load power output with respect to temperature differences. Comparing these graphs with Fig. 4, it is clear that the voltage and current output decrease after adding load resistance and thus output power decreases.

3.2 Double TEG Module

In this case, two back-to-back TEG modules were connected in series to increase the output voltage. Fig. 6 shows the configuration of double TEG modules. Same steps were followed to get the open circuit voltage, short circuit current, power and then load voltage, load current, load power.

Fig. 7 and Fig. 8 represent open circuit voltage, short circuit current and power, and load voltage, load current and load power, respectively, with respect to temperature differences. The voltage, current, and power output is more than single TEG module.

Comparing Fig. 7(b) with Fig. 8(b), the power output is almost double at matched load at maximum temperature difference. It is because of two back-to-back modules were connected in series, which increases the thermal resistance of the modules between two surfaces and also increases the thickness of the module. Therefore, the temperature difference between two surfaces was more than one module, which increases the output power as well. Figure 9 shows the temperature difference between single and double TEG modules with respect temperature difference between hot side and ambient.

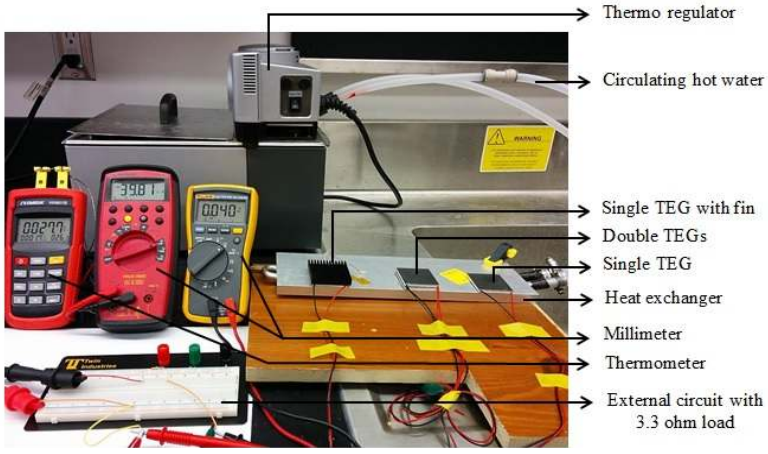

Fig. 2. Experimental setup

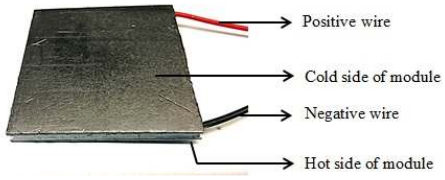

Fig. 3. Single TEG module

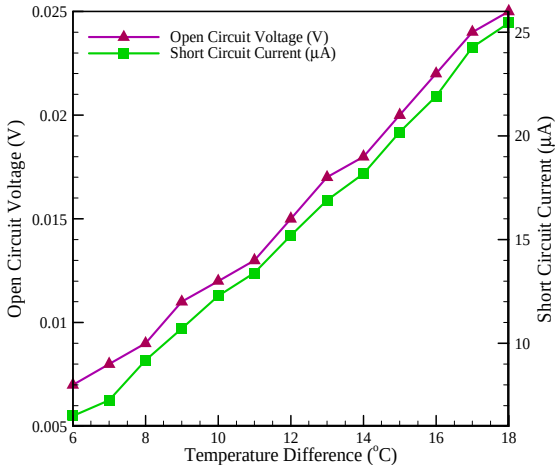

(a)

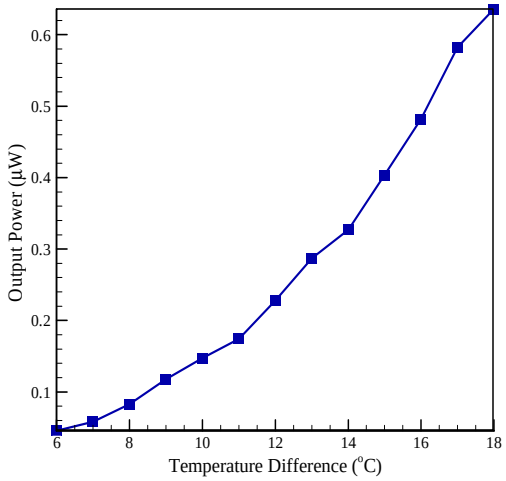

(b)

Fig. 4. (a) Open circuit voltage and short circuit current and (b) Output power with respect to the temperature difference between the hot and ambient temperature for a single module

3.3 Single TEG Module with Fin

Finally, a fin of size 45.97 mm × 45.97 mm × 9.02 mm was attached to the cold surface of TEG. Usually, the fin is used to increase the heat dissipation rate from any hot surface. The thermal heat energy goes parallel from a hot surface to cold surface and increases the temperature of cold surface gradually. At the same time, the heat dissipates from the cold surface to the surrounding environment through convection process. If the fin is attached then this dissipation rate will be increased. Fig. 10 shows the arrangements of the set-up of the fin with a single module.

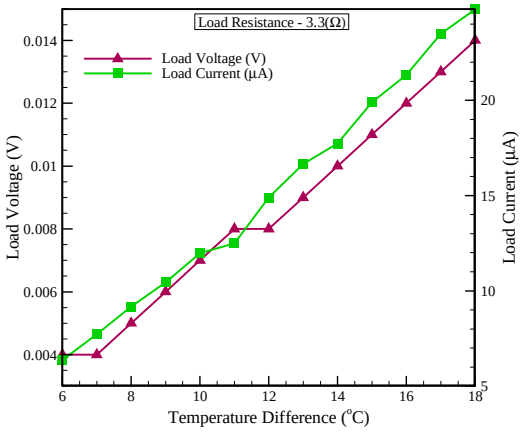

(a)

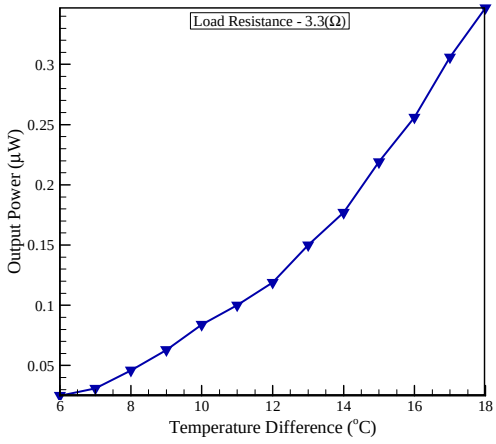

(b)

Fig. 5. (a) Load voltage and Load current, (b) Output power with respect to the temperature difference between the hot and ambient temperature for a single module

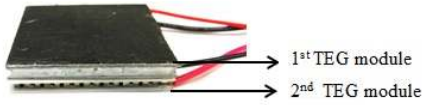

Fig. 6. Double TEG modules

Fig. 11 and Fig. 12 illustrate voltage, current and power output without and with load resistance,

respectively, against the temperature differences. It is noticeable that output voltage, current and power is more than previous two cases.

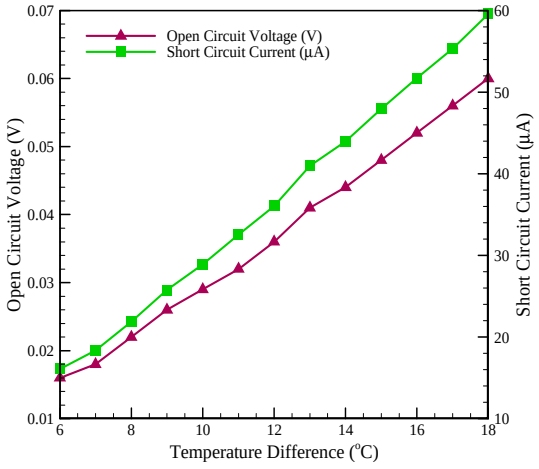

(a)

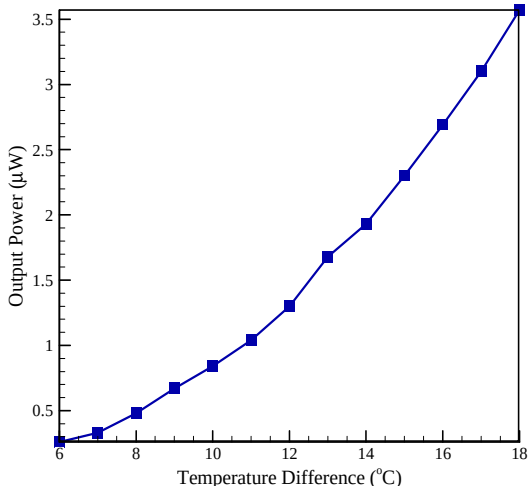

(b)

Fig. 7. (a) Open circuit voltage and short circuit current (b) Output power with respect to temperature for double modules

Comparing these three different cases, the single TEG with fin is more suitable then only single and double TEG configurations. Fig. 13 indicates the output power for three different cases at matched load. Considering wearable TEG, it should be small, light, and thin. In that case, double TEG configuration is suitable as it is thinner but the output power is not higher than a single TEG with fin configuration. However, the price of TEG module is also quite higher than a fin. In the double module, another problem may occur if one of the modules becomes inactive then the output power will become zero. Therefore, the single TEG with a fin can be considered the suitable one for power harvesting from the human body.

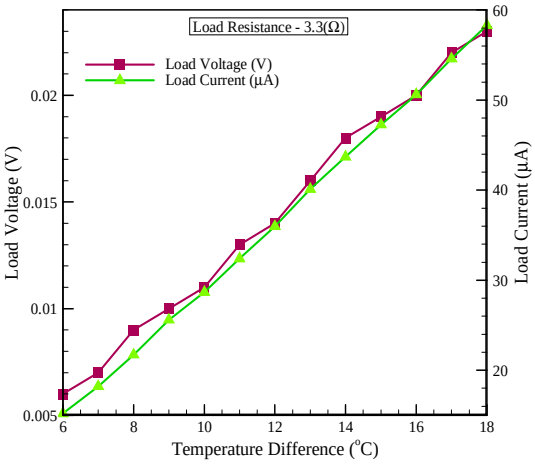

(a)

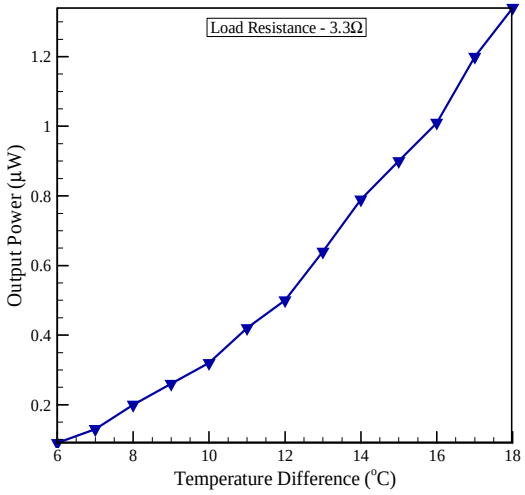

(b)

Fig. 8. (a) Load voltage and load current, and (b) Output power with respect to temperature difference for double modules

Figs. 14 and 15 show the experimental set-up and test results of TEG attached to the arm at different conditions i.e., single TEG, single TEG beside window, single TEG with heat sink, single TEG with heat sink beside window.

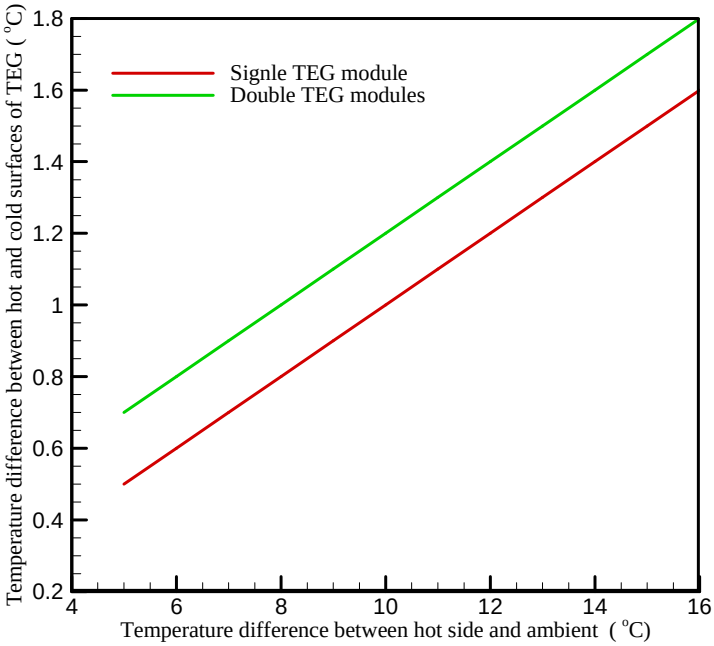

Fig. 9. Temperature difference between hot and cold surface along with temperature difference between hot side and ambient of single and double TEG modules, respectively

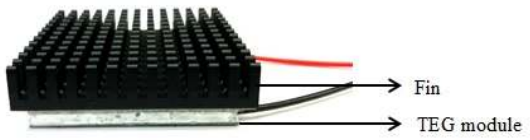

Fig. 10. Single TEG module with fin

4. ANALYSIS OF THERMOELECTRIC MATERIALS

The module, which is used for the experiment, is not suitable for a low-temperature environment. Therefore, it is important to find out thermoelectric materials those have a good material profile to work at low temperature, must be used in TE module for the wearable thermoelectric generator. Most of the cases, Bi_2Te_3 and Bi_2Se_3 are used for low-temperature applications in TEGs [2]. Now researchers are trying to modify these material properties and mixing with other nanomaterials to increase the figure of merit (*Z*).

4.1 Low Temperature Based Materials

There are different n-type and p-type semiconductor materials available to be used, but most of the materials have a high-temperature profile. For wearable applications, the temperature range is ΔT=6-18 K, where the body and ambient temperatures are 37℃ and 19-31℃, respectively. The hot side and cold side temperatures are considered as 310 K and 298 K. Therefore, the average temperature of these two surfaces is 304 K, which is considered for investigating the materials properties. To find such materials for this temperature range, different handbooks are studied and listed the suitable materials in Table 2.

From Table 2, n-type 75% Bi_2Te_3, 25% Bi_2Se_3 and p-type 25% Bi_2Te_3 0.75% Sb_2Te_3 (1.75%Se) were considered for further numerical and finite element analysis due to their high figure of merit for wearable TEG.

4.2 Numerical Analysis

According to Eqs. (4) and (5), the rate of heat flow going in and out from the TEG surface is given by:

$$\dot{Q}_H = n[\alpha I T_{Hs} + K(T_{Hs} - T_{Cs}) - 0.5 I^2 R_{in}] \quad (4)$$

$$\dot{Q}_C = n[\alpha I T_{Cs} + K(T_{Hs} - T_{Cs}) + 0.5 I^2 R_{in}] \quad (5)$$

In these equations, almost all parameters are known except T_{Hs} and T_{Cs} temperatures.

Actually, T_{Hs} is not equal to the hot side temperature of T_H and similarly T_{Cs} in not equal to T_{air}, which is the cold side. Theoretically, the rate of heat flow at the hot side must be equal to the rate of heat flow at the hot surface of the element and similarly for the cold surface. However, practically there is some heat loss as heat convection, which also must be equal to the rate of flow of heat from the hot surface to the cold surface of the element. Fig. 16 illustrates the schematic diagram of a practical scenario of heat flow from hot side to cold side of a TEG.

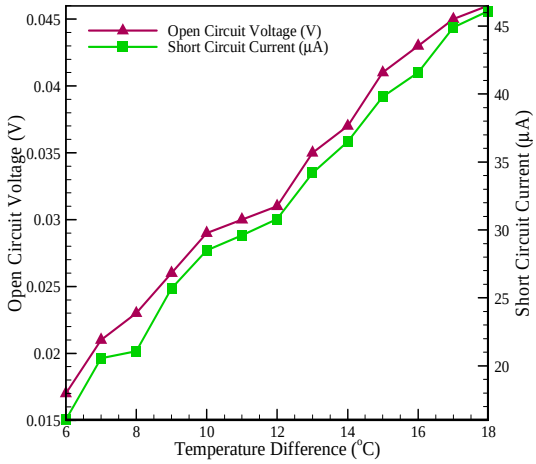

(a)

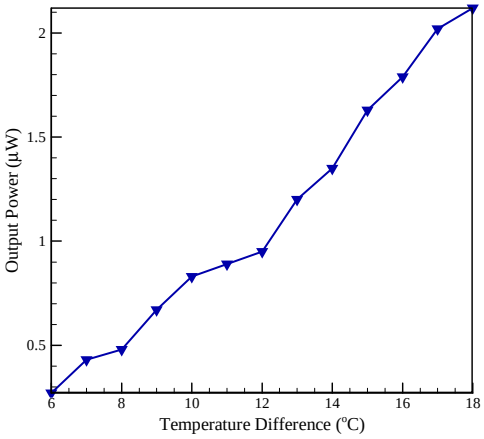

(b)

Fig. 11. (a) Open circuit voltage and short circuit current, (b) Output power with respect to the temperature difference

For the simplicity of numerical analysis of the module, following assumptions are made:

(i) The whole system is in steady state;
(ii) The properties of the TE materials are independent of temperature changes;
(iii) The size and dimensions of all n-type and p-type elements are identical;
(iv) The TE elements are connected in series and heat flows parallel from hot to cold side;
(v) The surroundings of the n-type and p-type materials (left, right and the gap between them) are adiabatic.

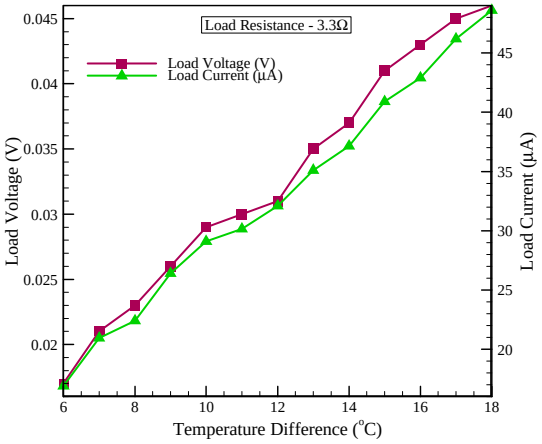

(a)

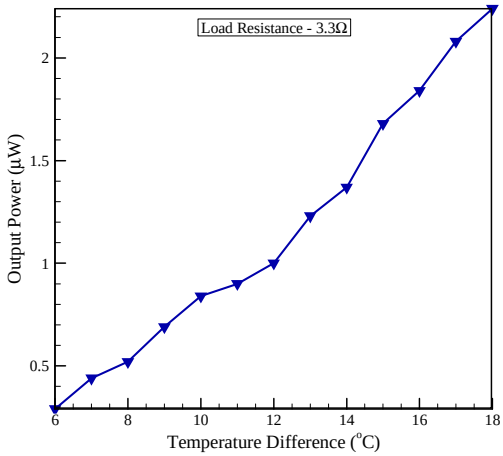

(b)

Fig. 12. (a) Load voltage and Load current, (b) Output power with respect to temperature difference at R_L=3.3 Ω

Now considering the heat convection process, the rate of heat flow from hot side to hot surface of the element and cold surface to ambient temperature are given by:

$$\dot{Q}_H = h_1 A_1 (T_H - T_{Hs}) \quad (9)$$

$$\dot{Q}_C = h_2 A_2 (T_{Cs} - T_{air}) \quad (10)$$

According to Eqs. (4), (5) and Eqs. (9), (10), the rate of heat flow is rewritten as:

$$\dot{Q}_H = n[\alpha I T_{Hs} + K(T_{Hs} - T_{Cs}) - 0.5 I^2 R_{in}] = h_1 A_1 (T_H - T_{Hs}) \quad (11)$$

$$\dot{Q}_C = n[\alpha I T_{Cs} + K(T_{Hs} - T_{Cs}) + 0.5 I^2 R_{in}] = h_2 A_2 (T_{Cs} - T_{air}) \quad (12)$$

where, h_1 (assumed for numerical analysis 0.5 W/m^{2}K) and A_1 (0.054 mm^2) are the heat transfer coefficient and surface area of the upper copper plate, respectively. Similarly, h_2 (assumed 0.035 W/m^{2}K) and A_2 (0.0392 mm^2) are the heat transfer coefficient and surface area of the lower copper plate, respectively. When $h_1 A_1 = h_2 A_2 =$ infinity only that case $T_H = T_{Hs}$ and $T_{Cs} = T_{air}$ which is not practically possible. Solving the Eqs. (11) and (12), unknown parameters T_{Hs} and T_{Cs} can be found as:

$$T_{Hs} = \frac{(nK - n\alpha I + h_2 A_2)(0.5 n I^2 R_{in} + h_1 A_1 T_H) + (0.5 n I^2 R_{in} + h_2 A_2 T_{air}) nK}{(h_1 A_1 + nK + n\alpha I)(nK - n\alpha I + h_2 A_2) - (nk)^2} \quad (13)$$

$$T_{Cs} = -\frac{nK(-0.5 n I^2 R_{in} - h_1 A_1 T_H) + (-h_1 A_1 - nK - n\alpha I)(0.5 n I^2 R_{in} + h_2 A_2 T_{air})}{(h_1 A_1 + nK + n\alpha I)(nK - n\alpha I + h_2 A_2) - (nK)^2} \quad (14)$$

Substitute Eqs. (13) and (14) into Eqs. (4) and (5) to calculate the heat flow rates and then output power can be easily calculated from Eq. (3). For numerical analysis, material properties were taken from Table 2, and the size and dimensions are taken from Table 1 where, T_H=310 K, T_{air}=298 K. The whole numerical analysis was carried out in Maple software to get the power. Fig. 17 illustrates the output results in the output power with respect to the load current. The temperature difference between T_{Hs} and T_{Cs} (i.e., the difference was around 3 K calculated from theoretical analysis) was very low which was one of the main reasons of low power output (µW level). The output power increases with increasing electrical current. However reaching the peak value, the power output decreases with further increasing of current. The theoretical maximum power is calculated to be 6.5 µW at 0.015 A with ΔT of 3 K.

4.3 Finite Element Analysis (FEA)

Finite element analysis was done in FlexPDE software using the materials properties and geometry. Fig. 18 shows the mesh analysis of TE element. In this analysis, an external load was added at the bottom to complete the cycle. The electrical resistance of the load was equal to the internal resistance of the thermoelectric material.

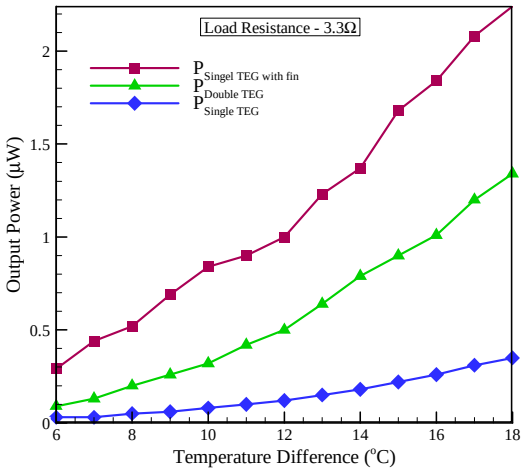

Fig. 13. Output power for three different configurations

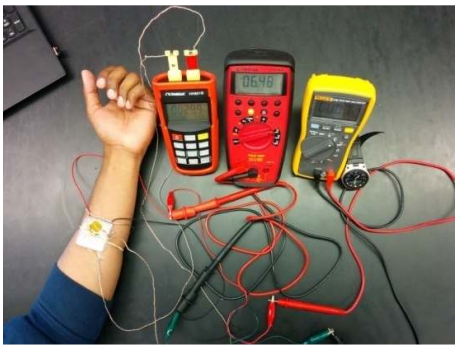

(a)

(b)

Fig. 14. (a) Single TEG and (b) TEG with heat sink attached to arm

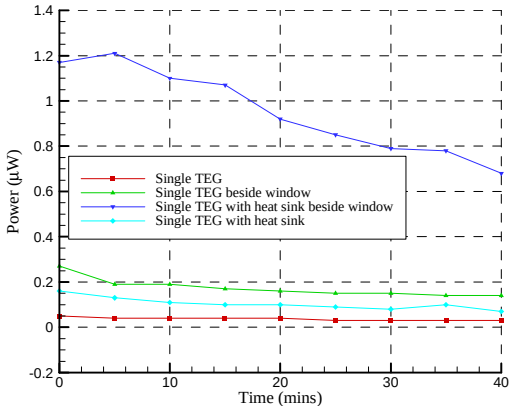

Fig. 15. Power output from TEG attached to the arm at different conditions

4.3.1 Governing equation for FEA

The governing equations for electric field ($\vec{E}$) produced in the thermoelectric element due to the temperature difference (ΔT) and heat flow ($\vec{q}$) through the elements due to the Peltier effect, are given by:

$$\vec{J} = \sigma(\vec{E} - \alpha\Delta T) \quad (15)$$

$$\vec{q} = \alpha T\vec{J} - k\Delta T \quad (16)$$

here, $\vec{J}$, σ, α, k are current density, electrical conductivity, Seebeck coefficient, and thermal conductivity, respectively. According to the conservation principle of energy and current:

$$\nabla.\vec{q} = \vec{J}.\vec{E} = \dot{q} \quad (17)$$

$$\nabla.\vec{J} = 0 \quad (18)$$

According to the definition of electric potential, electric field is given by:

$$\vec{E} = -\nabla V \quad (19)$$

Fig. 19 represents heat flow, current density profiles of designed TE pair. Fig. 19 (a) shows that the heat flows from hot surface (T_{Hs}=310 K) to cold surface (T_{Cs}=306 K) but not flowing through the gap between legs, sidewalls, and not also through the load, as it is not the part of the TEG.

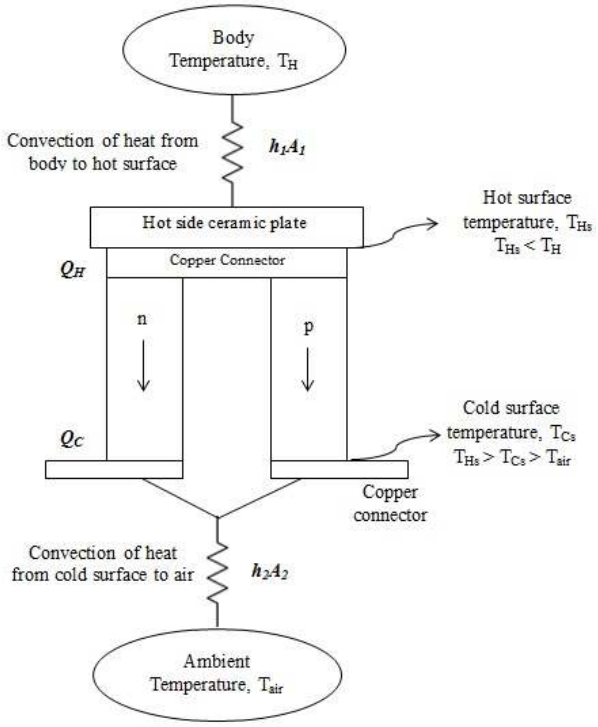

Fig. 16. Schematic diagram of heat flow in and out from a TE element

Table 2. The *n*-type and *p*-type TE material properties at low temperature [21,22]

Type	Material	Seebeck coefficient, 10^{-6} (V/K)	Electrical resistivity (10^{-3} ohm-cm)	Figure of merit (10^{-3} K^{-1})
n-type	75% Bi_2Te_3, 25% Bi_2Se_3	-159.2	1.02	2.03
	Bismuth telluride ($Bi_{1.75}Te_{3.25}$)-sulfur ball milled	-110	6	0.23
p-type	25% Bi_2Te_3 0.75% Sb_2Te_3 (1.75%Se)	201	1.03	3.47
	$AgSbTe_2$	204.2857	4.9	1.13
	$Si_{0.7}Ge_{0.3}$	221.1111	4.02	0.19
	TAGS-85-($AgSbTe_2$)1-85,(GeTe)85	78.08	0.68	0.68
	Antimony telluride (Sb_2Te_3) sulfur ball milled	120	0.002	0.82

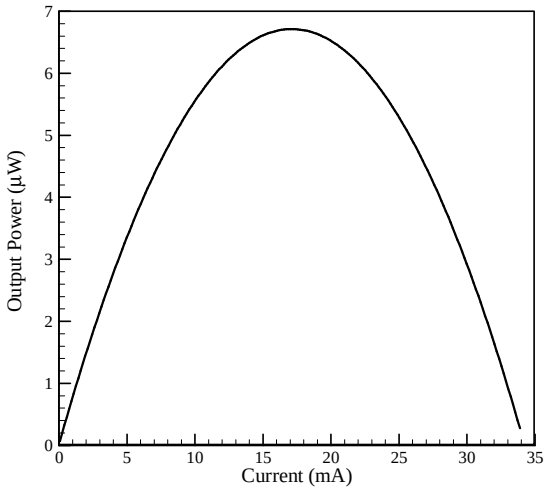

Fig. 17. Theoretical result of the power output with respect to current

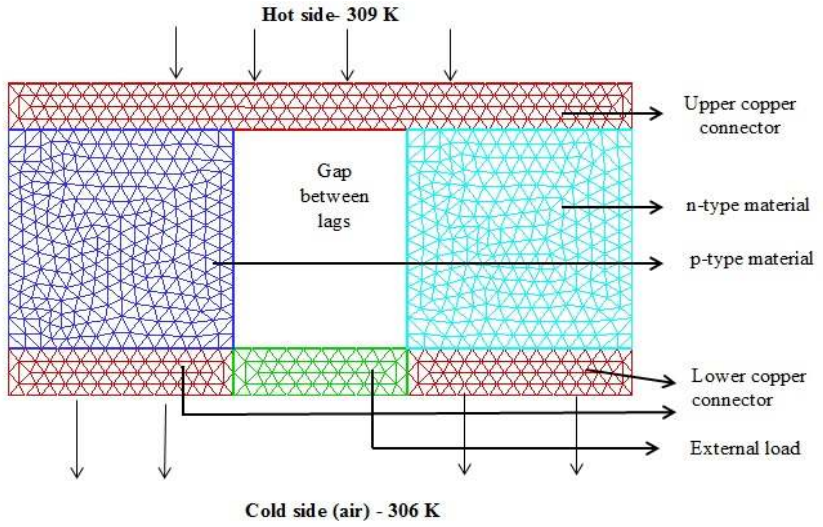

Fig. 18. Mesh analysis of TE element

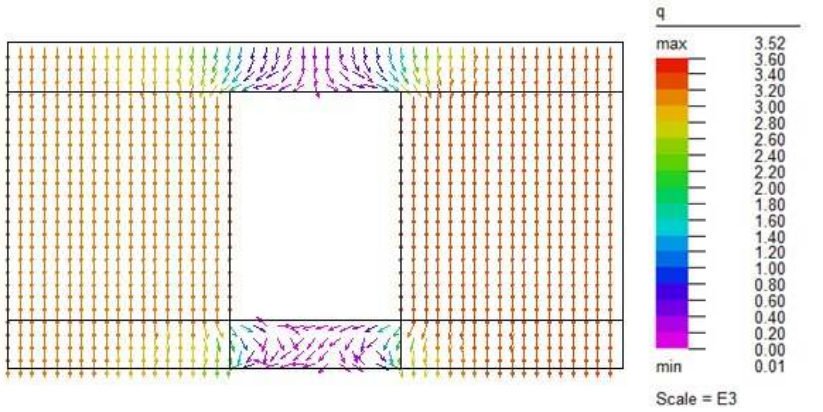

(a)

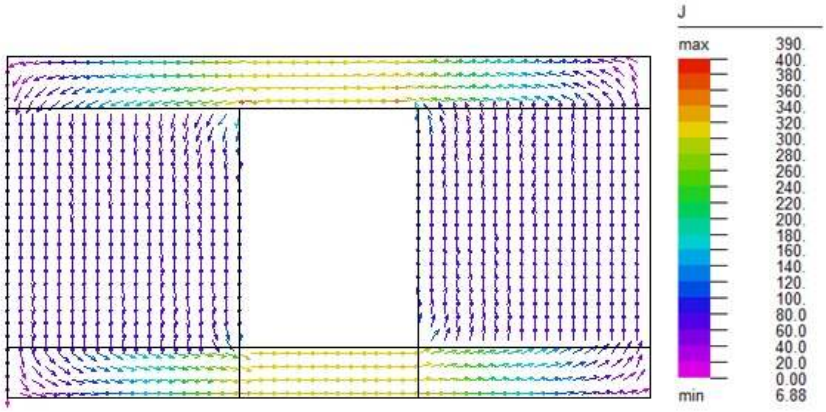

(b)

Fig. 19. (a) heat flow profile and (b) current density profile of a single TE module

Fig. 20. Typical TEG module attached on body

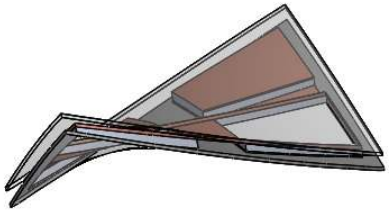

(a)

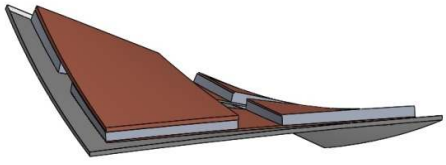

(b)

Fig. 21. The flexibility of wearable TEG

5. CHALLENGES OF GENERATING OPTIMUM POWER

Most of the wearable TEGs generate power of micro (μ) watt range even less than this. It becomes a challenge to generate optimum energy to power up the mobile electronic devices from this green technology. Some existing challenges are discussed below:

(i) Low Thermal Resistance [23].
(ii) Low figure of merit of TE materials [2].
(iii) The flexibility of Module: Flexibility of the module is another big problem. The TEG modules that are available in the market have a rigid body at the top and bottom side. However, the human body is not a plain surface. The body has different shapes and curves. Fig. 20 shows an overview of the human curved body with a rigid TEG. Therefore, TEGs are not attached to the body very tightly which reduces heat flow from the body to the hot

surface of the module. Fig. 21 presents a flexible TEG module designed in SolidWorks.

6. CONCLUSION

In this paper, both theoretical and experimental analyses have been described. Experimental work was carried out using an existing TEG module. A maximum output power of 0.35 µW was measured for the single module at matched load. Double and single modules with fin were also tried for the experiment. Therefore, it was found that the among these three configurations, single TEG with a fin has a high power output of around 2.5 µW, which is nearly 7 times greater than a single module. In theoretical analysis, *n*-type 75% Bi_2Te_3, 25% Bi_2Se_3 and *p*-type 25% Bi_2Te_3 0.75% Sb_2Te_3 (1.75%Se) were used. The theoretical result shows that TEG with these TE materials generates approximately 6.5 µW when ΔT is 3 K. Finite element analysis of n-type and p-type materials shows their heat flow and current density profile when the hot surface and cold surface temperature are 310 K and 306 K, respectively.

Now flexibility and high power output are two main concerns for the further developments of WTEG for researchers. To optimize the output power and make the WTEG module more flexible and thin, the existing challenges might be considered to overcome the problems as a future work.

ACKNOWLEDGEMENT

This project was partially funded through the internal funding of Deanship of Research of University of Tabuk within the project number S-1436-0242. The authors also thankful to Dr. Shohel Mahmud, Department of Mechanical Engineering, University of Guelph for the laboratory and equipment support of Advanced Energy Conversion & Control Lab.

COMPETING INTERESTS

Authors have declared that no competing interests exist.

REFERENCES

1. Xi H, Luo L, Fraisse G. Development and applications of solar-based thermoelectric technologies. Renew Sustain Energy Rev. 2007;11:923–36.
2. Siddique ARM, Mahmud S, Heyst BV. A comprehensive review on vibration based micro power generators using electromagnetic and piezoelectric transducer mechanisms. Energy Conversion and Management. 2015; 106:728–747.
3. Omer AM. Focus on low carbon technologies: The positive solution. Renew Sustain Energy Rev. 2008;12:2331–57.
4. Gould C, Shammas N. A review of thermoelectric mems devices for micro-power generation, heating and cooling applications. Micro Electronic and Mechanical Systems, Kenichi Takahata (Ed.); 2008.
ISBN: 978-953-307-027-8
5. Leonov V, Torfs T, Vullers RJM, Su J, Hoof CV. Renewable energy microsystems integrated in maintenance-free wearable and textile-based devices: The capabilities and challenges. IEEE. 2010;967-972.
6. Leonov V, Vullers RJM. Wearable electronics self-powered by using human body heat: The state of the art and the perspective. Journal of Renewable and Sustainable Energy. 2009;062701:1-14.
7. Mitcheson PD. Energy harvesting for human wearable and implantable bio-sensors. 32nd Annual International Conference of the IEEE EMBS. 2010;3432-3436.
8. Lossec M, Multon B, Ahmed HB, Goupil C. Thermoelectric generator placed on the human body: System modeling and energy conversion improvements. Eur. Phys. J. Appl. Phys. 2010;52(11103):1-10.
9. Leonov V. Thermoelectric energy harvester on the heated human machine. J. Micromech. Microeng. 2011; 21,125013:1-8.
10. Jo SE, Kim MK, Kim MS, Kim YJ. Flexible thermoelectric generator for human body heat energy harvesting. Electronics Letters. 2012;48(16).
11. Suemori K, Hoshino S, Kamata T. Flexible and lightweight thermoelectric generators composed of carbon nanotube–polystyrene composites printed on film substrate. Applied Physics Letters. 2013; 103(153902):1-4.
12. Kim MK, Kim MS, Lee S, Kim C, Kim YJ. Wearable thermoelectric generator for harvesting human body heat energy. Smart Mater. Struct. 2014;23(105002):1-7.
13. Kim SJ, We JH, Cho BJ. A wearable thermoelectric generator fabricated on a

glass fabric. Energy Environ. Sci. 2014;7:1959–1965.

14. Gould CA, Shammas NYA, Grainger S, Taylor I. A comprehensive review of thermoelectric technology, micro-electrical and power generation properties. PROC. 26th International Conference on Microelectronics (MIEL 2008). 2008;329-332.
15. Tan J, Kalantar-zadeh K, Wlodarski W, Bhargava S, Akolekar D, Holland A, Rosengarten G. Thermoelectric properties of bismuth telluride thin films deposited by radio frequency magnetron sputtering. Proc. SPIE 5836, Smart Sensors, Actuators, and MEMS II. 2005.
16. Zheng Z, Fan P, Luo J, Liang G, Zhang D. Enhanced thermoelectric properties of antimony telluride thin films with preferred orientation prepared by sputtering a fan-shaped binary composite target. Journal of Electronic Materials. 2013;42:3421-3425.
17. Ahıska R, Mamur H. A review: Thermoelectric generators in renewable energy. International Journal of Renewable Energy Research. 2014;4(1):128-136.
18. Franciosoa L, Pascali CD, Farella I, Martuccia C, Cretì P, Siciliano P, Perrone A. Flexible thermoelectric generator for ambient assisted living wearable biometric sensors. Journal of Power Sources. 2011; 196:3239–3243.
19. Terry MT, Subramanian MA. Thermoelectric materials, phenomena and applications: A bird's eye view. MRS Bulletin. 2011;31(3):188.
20. Tellurex Inc; 2015.
Available:http://tellurex.com/shop-products/
(Accessed: 05.10.15)
21. Rowe DM. CRC handbook of thermoelectric; 1995.
ISBN 0-8493-0146-7
22. Rosi FD, Hocking EF, Lindenblad NE. Semiconductor power generation. RCA Review, XXII; 1961.
23. Wang Z, Leonov V, Fiorini P, Hoof CV. Micromachined thermopiles for energy scavenging on human body. 14th International Conference on Solid-State Sensors, Actuators and Microsystems; 2007.

Peer-review history:
The peer review history for this paper can be accessed here:
http://sciencedomain.org/review-history/15739